

Global Biogeochemical Cycles



RESEARCH ARTICLE

10.1029/2018GB005967

Key Points:

- Surface sediments of the Laptev and East Siberian Sea contain 2.7 Tg terrigenous organic carbon (terrOC) of which 55% resist degradation
- Integrating cross-shelf terrOC losses with millennial transport times yield degradation fluxes of about 1.7 Gg (= 1,700 t) carbon per year
- Degradation of terrOC in sediments is orders of magnitude smaller than estimates for degradation in the water column

Supporting Information:

- Supporting Information S1

Correspondence to:

L. Bröder and Ö. Gustafsson,
l.m.broeder@vu.nl;
orjan.gustafsson@aces.su.se

Citation:

Bröder, L., Andersson, A., Tesi, T., Semiletov, I., & Gustafsson, Ö. (2019). Quantifying degradative loss of terrigenous organic carbon in surface sediments across the Laptev and East Siberian Sea. *Global Biogeochemical Cycles*, 33, 85–99. <https://doi.org/10.1029/2018GB005967>





Received 25 APR 2018

Accepted 17 DEC 2018

Accepted article online 5 JAN 2019

Published online 28 JAN 2019

Quantifying Degradative Loss of Terrigenous Organic Carbon in Surface Sediments Across the Laptev and East Siberian Sea

Lisa Bröder^{1,2,3} , August Andersson^{1,2} , Tommaso Tesi⁴ , Igor Semiletov^{5,6,7}, and Örjan Gustafsson^{1,2} 

¹Department of Environmental Science and Analytical Chemistry, Stockholm University, Stockholm, Sweden, ²Bolin Centre for Climate Research, Stockholm University, Stockholm, Sweden, ³Department of Earth Sciences, Vrije Universiteit Amsterdam, Amsterdam, Netherlands, ⁴Institute of Marine Sciences – National Research Council, Bologna, Italy, ⁵International Arctic Research Center, University Alaska Fairbanks, Fairbanks, USA, ⁶Pacific Oceanological Institute, Russian Academy of Sciences, Vladivostok, Russia, ⁷National Research Tomsk Polytechnic University, Tomsk, Russia

Abstract Ongoing permafrost thaw in the Arctic may remobilize large amounts of old organic matter. Upon transport to the Siberian shelf seas, this material may be degraded and released to the atmosphere, exported off-shelf, or buried in the sediments. While our understanding of the fate of permafrost-derived organic matter in shelf waters is improving, poor constraints remain regarding degradation in sediments. Here we use an extensive data set of organic carbon concentrations and isotopes ($n = 109$) to inventory terrigenous organic carbon (terrOC) in surficial sediments of the Laptev and East Siberian Seas (LS + ESS). Of these ~2.7 Tg terrOC about 55% appear resistant to degradation on a millennial timescale. A first-order degradation rate constant of 1.5 kyr^{-1} is derived by combining a previously established relationship between water depth and cross-shelf sediment-terrOC transport time with mineral-associated terrOC loadings. This yields a terrOC degradation flux of ~1.7 Gg/year from surficial sediments during cross-shelf transport, which is orders of magnitude lower than earlier estimates for degradation fluxes of dissolved and particulate terrOC in the water column of the LS + ESS. The difference is mainly due to the low degradation rate constant of sedimentary terrOC, likely caused by a combination of factors: (i) the lower availability of oxygen in the sediments compared to fully oxygenated waters, (ii) the stabilizing role of terrOC-mineral associations, and (iii) the higher proportion of material that is intrinsically recalcitrant due to its chemical/molecular structure in sediments. Sequestration of permafrost-released terrOC in shelf sediments may thereby attenuate the otherwise expected permafrost carbon-climate feedback.

Plain language summary Frozen soils in the Arctic contain large amounts of old organic matter. With ongoing climate change this previously freeze-locked carbon storage becomes vulnerable to transport and decay. Upon delivery to the shallow nearshore seas, it may either be directly degraded to carbon dioxide or methane and thereby fuel further warming or get buried and stored in sediments on the sea floor. Our understanding of the fate of carbon released from permafrost soils is increasing, yet uncertainties remain regarding its degradation in the sediment. Here we constrain how much land-derived organic carbon is deposited in the top layer of the sediment (the part that is prone to transport and exposed to oxygen-stimulated degradation) in the Laptev and East Siberian Seas. We find that more than half of this stock likely resists degradation, while the rest decays relatively slowly. Therefore, the amount of carbon released annually from degradation in surface sediments is much smaller than what was found to be emitted from overlying waters in earlier studies. We suspect that this difference is caused by a combination of mechanisms hindering degradation in sediments and thus conclude that the burial of land-derived carbon may help to dampen the climate impact of thawing permafrost.

1. Introduction

Permafrost soils at high latitudes store vast amounts of organic carbon (OC). Current estimates constrain the soil OC content in the top 3 m of Arctic terrestrial permafrost to $1,035 \pm 150 \text{ Pg}$ (Hugelius et al., 2014), which is about half of the global soil OC reservoir. Amplified global warming for polar regions causes permafrost thaw and thus has the potential to remobilize these freeze-locked carbon stocks (Intergovernmental Panel

©2019. The Authors.

This is an open access article under the terms of the Creative Commons Attribution-NonCommercial-NoDerivs License, which permits use and distribution in any medium, provided the original work is properly cited, the use is non-commercial and no modifications or adaptations are made.

on Climate Change, 2013). The possible decomposition of this thawed organic matter to CO₂ or CH₄ and subsequent release to the atmosphere constitutes a positive feedback mechanism to ongoing climate warming (Schuur et al., 2015). However, not all remobilized soil OC is degraded at the place of thaw. For example, transport through rising river discharge with augmented sediment loads (Gordeev, 2006; McClelland et al., 2006; Savelieva et al., 2000; Syvitski, 2002) and direct input from accelerating coastal erosion (e.g., Günther et al., 2013) increases the delivery of permafrost-derived terrigenous OC (terrOC) to the Arctic Ocean. In the shallow Arctic shelf seas, terrOC can then either be remineralized in the water column or in shallow sediments or be buried deeper in the sediments, with the latter being a mechanism that could attenuate the otherwise expected carbon-climate feedback (Hilton et al., 2015; Vonk & Gustafsson, 2013).

Our current understanding of the fate of terrOC in the marine environment is lacking crucial pieces to properly assess the magnitude of this translocated permafrost carbon-climate feedback. Earlier studies demonstrated that terrOC degradation within the Laptev and East Siberian Sea shelves could play a significant role in the Arctic marine carbon cycle, as the microbial oxidation of terrOC may cause elevated CO₂ concentrations in the water column and consequent CO₂ release to the atmosphere (Anderson et al., 2009; Semiletov et al., 2004, 2007). The carbon fluxes related to degradation of terrOC in the water column and terrOC sequestration in sediments have been quantified in previous studies (Alling et al., 2010; Sánchez-García et al., 2011; Vonk et al., 2012). However, another vector of the larger-scale biogeochemical cycle, the degradation in the shallow sediment *reactor*, has not yet been quantitatively constrained for this, the World's largest, shelf sea system.

Earlier investigations of terrOC in Arctic margin surface sediments reported a strong decrease of terrigenous biomarker concentrations with increasing water depth/distance from the shore for the East Siberian Arctic Shelf (Bischoff et al., 2016; Bröder, Tesi, Salvadó, et al., 2016; Doğrul Selver et al., 2015; Sparkes et al., 2015, 2016; Tesi et al., 2014; Vonk et al., 2010) and parts of the North American Arctic margin (Goni et al., 2013). The extent of terrOC degradation appears to be depending on its exposure to oxygen, which in turn is a function of the sediment transport time (e.g., Keil et al., 2004; Mollenhauer et al., 2007). This has been confirmed by our recent study (Bröder et al., 2018), where we constrained the terrOC cross-shelf transport time for the wide Laptev Sea shelf to be $3,600 \pm 300$ years. By combining those results with the observed terrOC gradients along the Laptev Sea transect, we obtained first-order degradation rate constants for specific terrestrial biomarkers (lignin phenols, cutin acids, long-chain *n*-alkanes, and *n*-alkanoic acids), as well as for bulk terrOC, which was determined by a dual-carbon source apportionment strategy. The terrOC degradation rate constant for surface sediments was with $0.0022 \pm 0.0006 \text{ year}^{-1}$ three to four orders of magnitude smaller than degradation rate constants for the water column that had been determined earlier: 0.3 year^{-1} for dissolved OC (DOC; Alling et al., 2010) and $1.4 \pm 0.9 \text{ year}^{-1}$ for particulate OC (POC; Sánchez-García et al., 2011). Yet to assess the relative importance of the sedimentary reactor for terrOC degradation, we need to quantitatively compare the carbon fluxes that emerge from degradation in the sediment to those from the water column for the whole system rather than contrasting the different first-order degradation rates. This study therefore focuses on (1) constraining the inventory of terrOC in the sedimentary reactor, that is, the amount of terrOC in the mobile shallow sediments that is prone to degradation and not yet permanently buried (not including the bottom water POC/resuspended sediment just above the sediment-water interface or the deeper (anoxic) part of the sediments). These results will then be used to (2) estimate the carbon flux originating from degradation in the shallow sediment reactor and (3) quantitatively compare it to other OC fluxes for the Laptev and East Siberian Shelf Seas, such as the release from degradation in the suspended and dissolved phases, total input from land, total release to the atmosphere, and burial/sequestration in deeper parts of the sediment. To this end, we aim to achieve a more complete picture of ongoing processes governing terrOC fluxes on the vast Siberian shelves.

2. Materials and Methods

2.1. Study Area

The Laptev and the East Siberian Shelf Seas (LS + ESS) are situated between the Kara Sea and Severnaya Zemlya in the west and the Chuckchi Sea and Wrangel Island in the east. They cover an area of about 1,500,000 km² and have an average water depth of 55 m (Jakobsson et al., 2004). They make up the largest part of the East Siberian Arctic Shelf (which also includes the Russian part of the Chuckchi Sea), the widest

and shallowest shelf-sea system of the World. OC sources for the LS + ESS are largely terrigenous, stemming from coastal erosion and fluvial input, with comparably low marine primary production for most parts of the shelves due to limited light and nutrient availability (Sakshaug, 2004; Sánchez-García et al., 2011; Stein & Fahl, 2004; Vonk et al., 2012). The main fraction of OC in surface sediments originates from the destabilization of Pleistocene ice complex deposits (ICD) along the Siberian coastline. Different estimates for POC input from coastal erosion range between $4.0 \text{ Tg C year}^{-1}$ (Semiletov, 1999) and $22 \text{ Tg C year}^{-1}$ (Vonk et al., 2012). Riverine input is the second largest sediment source to the LS + ESS. Discharge from the large Siberian rivers Khatanga, Lena, Yana, Indigirka, and Kolyma (from west to east) has been approximated to add another $\sim 1.7 \text{ Tg C year}^{-1}$ of POC to the LS + ESS (Rachold et al., 2004). A new estimate for Lena and Kolyma Rivers downsized their POC delivery by 30%–60%, yielding a combined flux of $0.94 \text{ Tg C year}^{-1}$ (McClelland et al., 2016). The Lena River alone accounts for $\sim 70\%$ of the POC discharge to the LS + ESS. Its watershed expands over $2.46 \times 10^6 \text{ km}^2$ (Holmes et al., 2012), of which 77% are underlain by continuous permafrost (Amon et al., 2012).

Sediment transport mechanisms across the LS + ESS include storm-induced resuspension, the incorporation of suspended particulate matter in sea ice (Dethleff, 2005; Eicken et al., 1997), dense water formation as a result from brine ejection during freeze-up (Dethleff, 2010; Ivanov & Golovin, 2007), and ocean currents. The latter depend largely on the prevailing large-scale atmospheric conditions, that is, cyclonic or anticyclonic summer months. During positive phases of the Arctic Oscillation, (cyclonic) northerly winds predominate and strengthen the Siberian Coastal Current. The Lena River plume is then transported along the coast toward the East Siberian Sea. During negative phases of the Arctic Oscillation (anticyclonic) the primarily southerly winds drive Lena River water masses across the shelf toward the deep part of the Arctic Ocean (Charkin et al., 2011; Dmitrenko et al., 2008; Guay et al., 2001; Wegner et al., 2013; Weingartner et al., 1999). Sediment transport on Arctic shelves is strongly seasonal. The highest concentrations of suspended POC in the Laptev Sea are observed shortly after the spring flood, following river ice break up in May, and during late summer due to increased river bank erosion and primary production, while sediment transport slows down beneath the ice cover during winter (Semiletov et al., 2011; Wegner et al., 2005).

2.2. Sampling

New data for OC concentration, stable carbon isotopes ($\delta^{13}\text{C}$) and mineral surface area were generated for this study. They were combined with previously published data for these parameters to yield a total database of $n = 109$ sediment samples (Bröder, Tesi, Salvadó, et al., 2016; Bröder, Tesi, Andersson, et al., 2016; Vonk et al., 2012). These sediments were collected as part of the International Siberian Shelf Study (ISSS-08) expedition on board the R/V Yacob Smirnitskiy during summer 2008 and the Swedish-Russian-U.S. Investigation of Carbon-Climate-Cryosphere Interactions in the East Siberian Arctic Ocean (SWERUS-C3) expedition on I/B ODEN during summer 2014. Sediment cores were sampled with a GEMAX gravity corer (two Plexiglas tubes, 9-cm diameter) during ISSS-08 and with an Oktopus multicorer (eight Plexiglas tubes, 10-cm diameter) during SWERUS-C3. During ISSS-08, some samples were also collected with a Van Veen grab sampler. For the grab samples, only the uppermost $\sim 2 \text{ cm}$ were subsampled and used in this study. Sediment cores were cut into 1-cm slices within 24 hr after sampling. Only data for the top 0- to 1-cm slice were used in this study. All samples were kept frozen throughout the expedition and freeze-dried upon arrival to Stockholm University laboratories. For exact sampling locations and references to original publications see Table S1 in the supporting information.

2.3. Mineral Surface Area

All additional surface area (SA) analyses that are not part of previous publications (see Table S1 in the supporting information) have been performed on a Micromeritics Gemini VII Surface Area and Porosity analyzer. The organic material was removed from freeze-dried sediment subsamples ($\sim 0.7 \text{ g}$) by combustion at $400 \text{ }^\circ\text{C}$ for 12 hr. Salt and remaining ashes were removed by repeated mixing with MilliQ water ($\sim 50 \text{ ml}$) and centrifugation (20 min at 8,000 rpm), followed by further freeze-drying. Before analysis, the samples were degassed for 2 hr at $200 \text{ }^\circ\text{C}$ under a constant nitrogen flow in a Micromeritics FlowPrep 060 Sample Degas System. Prior to each analysis, the free space in the vial was measured. The specific surface areas were then derived from six pressure point measurements (with relative pressures $p/p_0 = 0.05\text{--}0.3$, equilibration time 5 s) with nitrogen as adsorbing gas following the method of Brunauer et al. (1938). The instrumental

error was 0.1–0.3 m²/g, which corresponds to a relative error of about 1%. The performance of the instrument was monitored with the surface area reference material carbon black (21.0 ± 0.75 m²/g) provided by Micromeritics and a TiO₂ reference material for lower surface areas (8.23 ± 0.21 m²/g).

2.4. Sediment Porosity and X-Ray Fluorescence (XRF)

Sediment core porosity was derived from gamma density measurements conducted with a Multi-Sensor Core Logger (Geotek, UK) on board I/B ODEN during the SWERUS-C3 2014 expedition. Nine entire cores with 10-cm diameter were used for analysis (see Table S1 in the supporting information for exact locations). Gamma rays were emitted from a ¹³⁷Cs source with energies at 0.662 MeV. Measurements were recorded with a resolution of 4 mm. The results were calibrated using a cylindrical piece of aluminum of varying thickness surrounded by water in a sealed liner, which was identical to those used for the sediment cores. The porosity Φ (defined as the volume not occupied by sediment particles, here saturated with water V_{water} , divided by the total volume V_{tot}) was calculated directly from the obtained wet bulk density data ρ_{bulk} .

$$\Phi \equiv \frac{V_{\text{water}}}{V_{\text{tot}}} = \frac{\rho_{\text{bulk}} - \rho_{\text{sed}}}{\rho_{\text{water}} - \rho_{\text{sed}}} \quad (1)$$

with sediment density $\rho_{\text{sed}} = 2.5 \text{ g/cm}^3$ and water density $\rho_{\text{water}} = 1.03 \text{ g/cm}^3$.

Three multicores (see Table S1 in the supporting information for exact locations) were scanned at the Core Processing Laboratory at the Department of Geological Sciences, Stockholm University, using an ITRAX core scanner (Cox Analytical Systems, Gothenburg, Sweden). This scan provides an optical digital image, a high-resolution X-ray digital image (supporting information Figure S1 for one representative sample), and micro-XRF elemental profiles for the elemental range from aluminum to uranium. For the XRF scans, a molybdenum tube (30 kV and 25 mA, dwell time 20 s) was used as a radiation source. The step size was set at 260 μm . Only lead concentrations are reported in this study (supporting information Figure S1). Acquired X-ray images were processed with in-house written Matlab scripts (Image Toolbox, MathWorks).

2.5. OC and Stable Carbon Isotopes ($\delta^{13}\text{C}$)

New data for OC concentrations and stable carbon isotopic composition ($\delta^{13}\text{C}$), added by this study to the growing total data set (see Table S1), were analyzed by the Stable Isotope Facility at the Department of Geological Sciences, Stockholm University. Freeze-dried, homogenized subsamples (~10 mg) were repeatedly acidified (HCl, 1.5 M) in Ag capsules to remove all inorganic carbon (Nieuwenhuize et al., 1994). The OC concentrations and $\delta^{13}\text{C}$ were measured simultaneously with a Carlo Erba NC2500 elemental analyzer connected via a split interface to a Finnigan MAT Delta V mass spectrometer. The OC concentrations were blank corrected by repeated analysis of empty Ag capsules. The relative error for OC concentrations was <1%. Stable isotope data are reported in $\delta^{13}\text{C}$ notation relative to VPDB.

2.6. Source Apportionment

The relative contributions of marine and terrigenous OC were quantified with an isotopic mass balance approach using $\delta^{13}\text{C}$ as a source marker. The marine $\delta^{13}\text{C}$ source signature was taken to be $-21 \pm 2.6\text{‰}$ and the terrigenous $-26.6 \pm 0.7\text{‰}$, following Tesi, Muschitiello, et al. (2016) with the terrigenous end-member here being the average of the two terrigenous end-members used in that study. Source proportions were estimated using a Markov Chain Monte Carlo approach. In general, terrOC may be divided into terrOC from the active layer (topsoil) and Pleistocene Ice-Complex Deposits (ICD) by combining $\delta^{13}\text{C}$ and $\Delta^{14}\text{C}$. However, establishing the topsoil $\Delta^{14}\text{C}$ endmember is complicated by the fact that it is influenced by the cross-shelf net transport time, which is so far only constrained for the eastern Laptev Sea (Bröder et al., 2018). One caveat of using only $\delta^{13}\text{C}$ as a source marker, on the other hand, is its relatively poorly constrained value for the marine end-member (e.g., Belicka & Harvey, 2009; Tesi et al., 2017), which is reflected in the comparatively large uncertainty of 2.6‰. The spread between marine and terrigenous sources, especially for ICD, is larger for $\Delta^{14}\text{C}$ ($-50\text{‰} \pm 12\text{‰}$ for marine, $-232\text{‰} \pm 147\text{‰}$ for topsoil and $-966\text{‰} \pm 45\text{‰}$ for ICD; Tesi, Muschitiello, et al., 2016), resulting in a higher precision of the dual carbon isotope approach. We therefore compared the estimated fraction terrOC from the single- and dual-isotope approaches for the Laptev Sea region (using the results from Bröder et al., 2018, for the dual-isotope source apportionment),

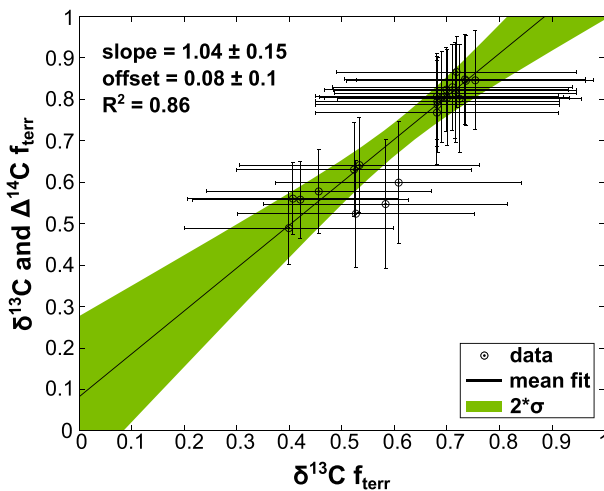


Figure 1. Comparison of the estimated fraction terrigenous organic carbon (f_{terr}) from the single ($\delta^{13}\text{C}$) and dual ($\delta^{13}\text{C}$ and $\Delta^{14}\text{C}$) isotope approaches: A linear relationship was fitted between the two predictions (including estimated uncertainties), which was used to correct all $\delta^{13}\text{C}$ -derived terrOC estimates.

noting that the fraction terrigenous (f_{terr}) is the sum of topsoil and ICD. A straight line was fitted between the two predictions (including estimated uncertainties), showing that the slope is 1, but there is a slight offset (see Figure 1). This fitted line was then used to correct all $\delta^{13}\text{C}$ -derived terrOC estimates. Another advantage of employing only $\delta^{13}\text{C}$ as a source marker (besides circumventing the poorly constrained topsoil $\Delta^{14}\text{C}$ value for the eastern part of the study area) was the greater coverage for $\delta^{13}\text{C}$ data than for $\Delta^{14}\text{C}$ data.

2.7. Correction for Sorting During Transport and Estimate of Transport Times

Larger particles (i.e., $>63\text{-}\mu\text{m}$ grain size) are mainly retained on the inner shelf due to hydrodynamic sorting (Tesi, Semiletov, et al., 2016). To quantify the mobile fraction of sedimentary terrOC (i.e., $<63\text{-}\mu\text{m}$ grain size; fine mineral-bound as opposed to coarse matrix-free plant debris), we used an empirical relationship (established in Bröder et al., 2018) between proportion TOC and water depth, based on a study by Tesi, Semiletov, et al. (2016), where the organic carbon distributions were measured in different sediment density, size, and settling velocity fractions for surface sediments from the East Siberian Arctic Shelf ($n = 9$). The dependency of the fraction fine on water depth is well described by fitting a logistic function (root-mean-square deviation of 0.052):

$$\text{Fraction fine [\%]} = \frac{100}{1 + 0.99 \cdot e^{-0.052 \cdot \text{water depth}}} \quad (2)$$

The fraction of sedimentary terrOC in fine sediments ($<63\ \mu\text{m}$) for each sample was thus calculated using the water depth at the sampling location, and this number then multiplied with the value for bulk terrOC to obtain the terrOC concentration for the fine fraction.

The transport times were determined according to the empirical relationship with depth established by Bröder et al. (2018):

$$\text{transport time (year)} = (42 \pm 3) \text{ year/m} \times \text{water depth (m)} \quad (3)$$

with water depths in m and transport times in years. This linear relationship was derived from compound-specific radiocarbon analysis on terrestrial biomarkers (long-chain fatty acids) from the mobile sediment fraction along a 600-km transect from the Lena River Delta across the Laptev Sea to the shelf edge. The inverse velocity of 42 ± 3 year/m was determined as a fitting parameter. The uncertainty of this parameters was accounted for by Monte Carlo simulations. A total of 1,000,000 iterations were run for each sample, with a burn-in (initial search) of 10,000 and a data thinning of 10 (rejecting all but every tenth result). See Table S2 in the supporting information for results.

2.8. Degradation Rate and Recalcitrant Fraction

The first-order degradation rate constant k (kyr^{-1}) for terrOC was obtained by fitting an exponential decay function with an offset to the terrOC loadings, terrOC , with regard to the transport time, t :

$$\text{terrOC}(t) = L_{\text{deg}} \cdot e^{-k \cdot t} + R \quad (4)$$

The offset, R (mg/m^2), defines the recalcitrant fraction of the terrOC, while L_{deg} (mg/m^2) describes the degradable fraction. Note that the SA-normalized terrOC loadings (instead of mass-normalized concentrations) were used for the degradation estimation. This is done in order to avoid masking the degradative loss by purely hydrodynamic processes such as particle size-dependent sorting during transport. Since we are focusing on the transport-prone terrOC fraction that is closely associated with mineral surfaces, this ambiguity can be prevented by normalizing to the mineral surface area of the sediments (e.g., Blair & Aller,

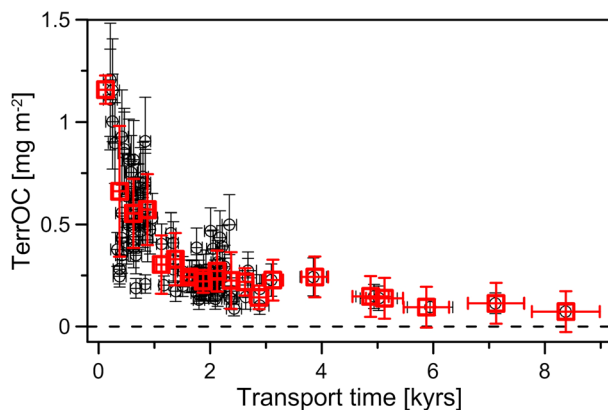


Figure 2. Relationship between transport time and terrigenous organic carbon (terrOC) loadings: Black open circles represent values of the individual samples (with standard deviations as error bars); red open squares are average values (with standard deviations) obtained by the binning of the samples into 250-year intervals.

2012; Keil et al., 1994). To assess the uncertainties of the fitting parameters, a Monte Carlo simulation was run also for this with 1,000,000 iterations, a burn-in of 10,000 and a data thinning of 10 (Table S2).

A complication with this approach is that there is a geographical bias for the data; many more data points were collected near shore, and thus with a shorter transport time. To account for this bias, the data points were binned in 250-year bins, and each bin was represented by the average and standard deviation for that bin (see Figure 2 and Table S3 in the supporting information). For bins with only one data point the standard deviation was estimated by the average standard deviation of all other bins.

2.9. Geographic Interpolation

A geographical interpolation of the terrOC concentrations (mg/gdw) was established over the study region to facilitate estimation of the terrOC inventory. The natural-neighbor approach was used, which is suitable for uneven distributions of data points. The interpolation was created on

a longitude-latitude grid with $1/60^\circ \times 1/60^\circ$ resolution. Given the spherical geometry, the amounts terrOC in each grid were scaled with the area of the grid when computing the total inventory.

3. Data

The hereby expanded data set on concentrations and related parameters gave insights on the spatial distributions and sources of organic carbon. The largest sources of organic matter on the LS + ESS are terrigenous resulting from the combination of low marine primary production (Sakshaug, 2004) and large river export and coastal erosion (McClelland et al., 2016; Vonk et al., 2012; see also section 2.1). This was reflected by the sedimentary OC concentrations (Figure 3a); highest values were found for samples close to the Lena River outlet and the coast (up to 26 mg/gdw, equivalent to 2.6 weight%), while OC concentrations on the outer shelf were generally low (3–7 mg/gdw). Some higher values were observed on the eastern outer shelf of the East Siberian Sea, likely stemming from increased marine production caused by nutrient-rich inflow of Pacific waters. The OC values agreed in magnitude and trends with other published work for the area (e.g., Fahl & Stein, 1997; Naidu et al., 2000; Semiletov et al., 2005; Shakhova et al., 2015).

The mineral SA is generally related to the grain size of the sediment particles with high values reflecting a finer mineral matrix and greater number of mesopores relative to coarse material (Mayer, 1994a). The SA commonly increases with distance from the coast, since the kinetic energy in the bottom waters decreases with increasing water depths; larger particles are therefore retained closer to the coast, while fine particles are more subject to winnowing-based transport. LS + ESS surface sediments by and large followed this trend, with values as low as 3.3 m²/gdw relatively close to the shoreline and the highest values (up to 39 m²/gdw) on the outer shelf (Figure 3b). There were, however, many exceptions of for example, fine sediments at shallow water depths or coarse material close to the shelf break (Figure 3b). The latter may be explained by winnowing of the fines across the shelf edge, leaving behind relatively coarse material.

The $\delta^{13}\text{C}$ signal of the organic material carries source information since marine primary production is generally less depleted (i.e., less negative) than land-derived organic matter (e.g., Fry & Sherr, 1984). Strong trends from about -27‰ close to the coast and the major river mouths up to about -21‰ on the outer shelf were visible (Figure 3c). These patterns are consistent with previous observations for the study area and neighboring Arctic shelves (e.g., Naidu et al., 2000; Semiletov et al., 2005).

4. Results

4.1. Distribution of OC and terrOC in Laptev and East Siberian Sea Surface Sediments

The distributions of OC and terrOC were interpolated across the LS + ESS using the compiled OC and $\delta^{13}\text{C}$ data (Figure 3). From these distributions, inventories of OC and terrOC were then derived. The boundaries of the enclosed area were dictated by the coverage of the samples and the 200-m isobar (slope $> 1^\circ$ at around

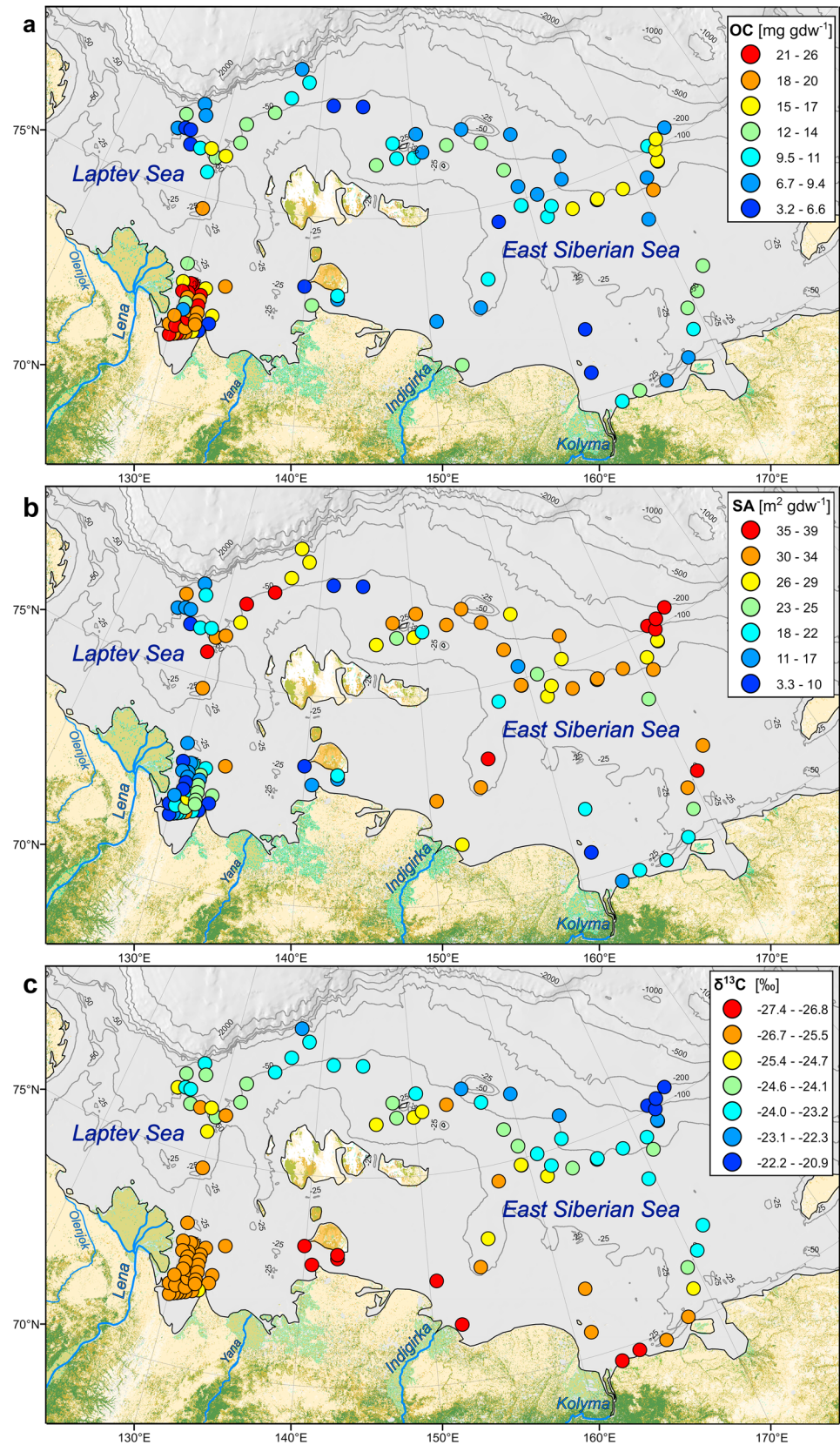


Figure 3. Surface sediment organic carbon concentrations (a), mineral surface area (b) and stable carbon isotope values (c).

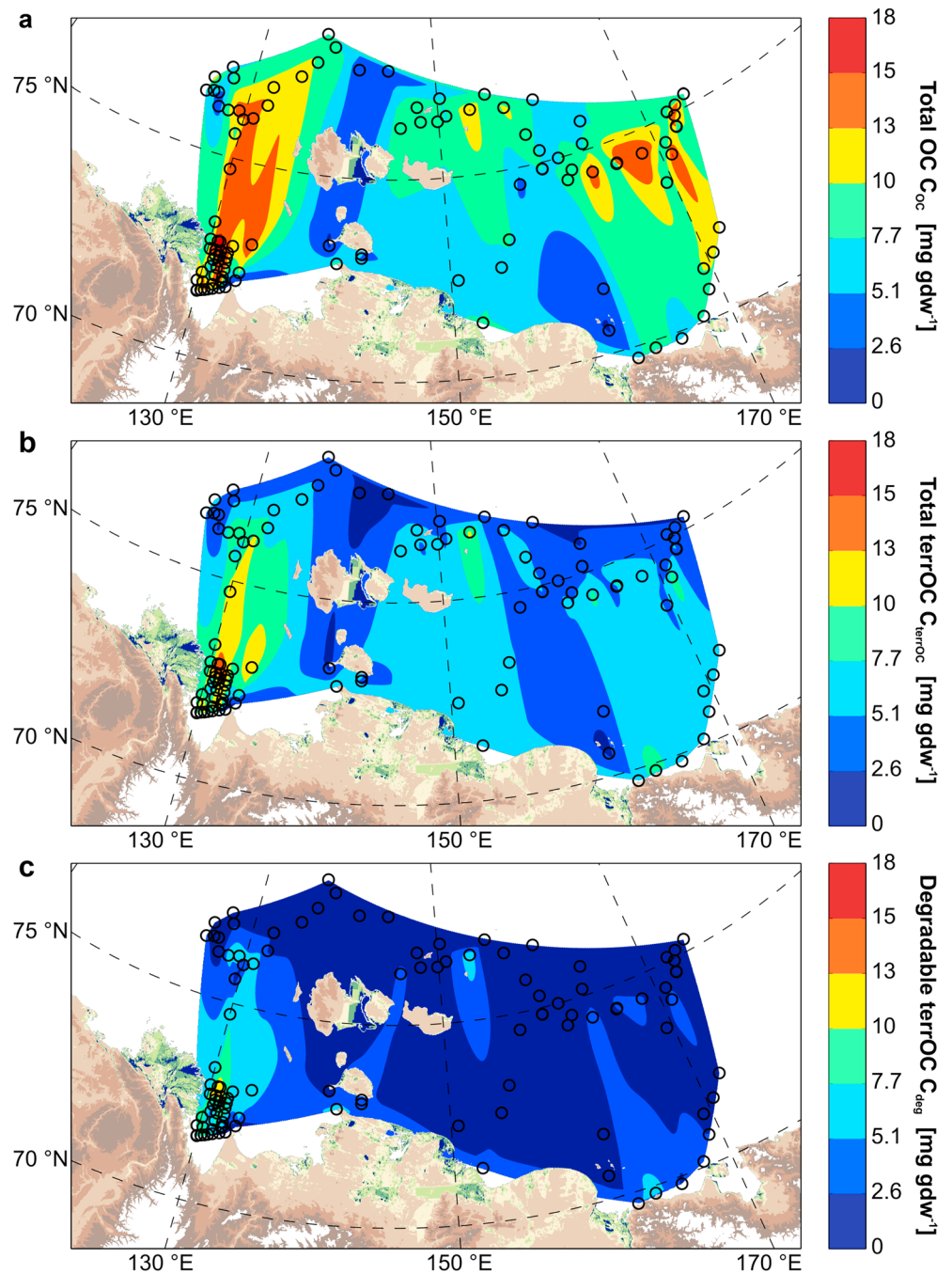


Figure 4. Maps of the Laptev Sea and East Siberian Sea (LS + ESS) with contour plots of the concentration of total organic carbon (OC; a), total terrigenous organic carbon (terrOC; b), and degradable terrOC (c), in the mobile fraction of the surface sediments. Open black circles refer to the sampling locations.

200-m water depth according to bathymetry analysis). The area covered by this approach is 816,000 km^2 , which corresponds to $\sim 55\%$ of the total LS + ESS shelf area ($\sim 1,500,000 \text{ km}^2$).

Since large particles are retained close to the coast and not transported across the shelf (Tesi, Semiletov, et al., 2016), we only account for the mobile fine fraction of the sediment ($< 63 \mu\text{m}$) that is subject to degradation during cross-shelf transport. The following concentrations were all corrected accordingly (see section 2.7 for details). The OC concentrations in the fine fraction spanned from 1.7 to 18 mg/gdw (Figure 4a and Table S2 in the supporting information). Two distinct areas with high such mass-

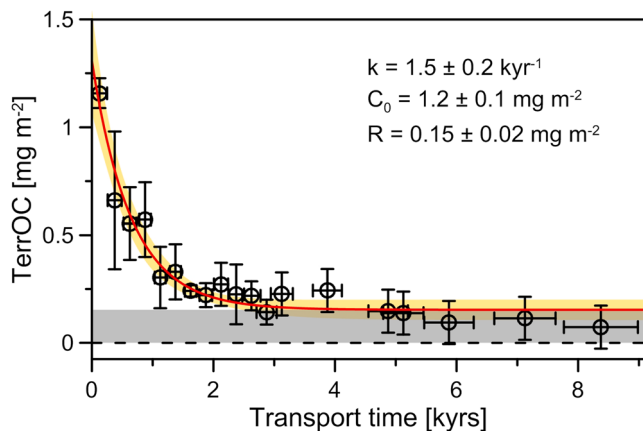


Figure 5. The relationship between terrigenous organic carbon (terrOC) loadings in the fine fraction and the cross-shelf transport time. Open symbols (and error bars) resemble the average (and standard deviation) of measured terrOC loadings within a bin of 0.25-kyr transport time (see also Figure 1 and section 2.8). The red line displays the fitted exponential decay function with the yellow-shaded area as the 2σ uncertainty of the fit and the gray shaded area as the asymptotic offset representing the recalcitrant residue (see text).

normalized OC concentrations were apparent; one north and east from the Lena River outlet and one on the outer eastern East Siberian Sea shelf.

The fraction terrOC of bulk OC calculated by $\delta^{13}\text{C}$ -based source apportionment ranged between 20%–80%. Higher proportions of terrOC were generally observed along the coast and north of the Lena River delta, while for the outer shelf, particularly in the ESS, terrOC contributions were considerably lower. These numbers and patterns are similar to previous estimates of the terrOC contribution in surface water POC (Semiletov et al., 2012). Total terrOC concentrations across the shelf ranged between 0.03 and 15 mg/gdw (Figure 4b and Table S2 in the supporting information). They were highest close to the Lena River delta and northward (roughly along 130°E). This also agrees with the patterns reported for terrestrial biomarkers such as lignin phenols (e.g., Bröder, Tesi, Andersson, et al., 2016; Karlsson et al., 2014; Tesi et al., 2014) and solvent-extractable lipids (e.g., Bischoff et al., 2016; Bröder, Tesi, Andersson, et al., 2016; Doğrul Selver et al., 2015; Karlsson et al., 2011, 2014; Sparkes et al., 2015). The comparison of the distribution of bulk OC with terrOC revealed that the high OC concentrations on the outer eastern East Siberian Sea shelf are probably to a large part caused by marine primary production, since terrOC concentrations in that area are rather low. This agrees with previous findings reporting the inflow of

nutrient-rich Pacific waters westward up to around 160°E (Anderson et al., 2011; Semiletov et al., 2005; Sparkes et al., 2016; Tesi et al., 2014).

4.2. Degradation Rate Constant

A first-order degradation rate constant was calculated from SA-normalized terrOC loadings and estimated transport times using a Monte-Carlo simulation strategy (see section 2.7 and 2.8 for details). Here in brief, the degradation rate constant is determined by fitting the following equation (4) to the data (Figure 5): $\text{terrOC}(t) = I_{\text{deg}} \cdot e^{-k \cdot t} + R$, with $\text{terrOC}(t)$ as SA-normalized terrOC loadings over transport time (t), I_{deg} the degradable terrOC loading ($I_{\text{deg}} = \text{terrOC}(0) - R$), and recalcitrant residue R . With this approach the bulk terrOC is considered, assuming a constant degradation rate for this entire carbon pool, rather than compound-specific degradation rates for single biomarkers. The degradation rate constant obtained for this complete data set (Figure 5) was with $1.5 \pm 0.2 \text{ kyr}^{-1}$ on the same order of magnitude but smaller than the one obtained for a Laptev Sea transect ($2.4 \pm 0.6 \text{ kyr}^{-1}$; Bröder et al., 2018). This difference may be caused by different source material for the Laptev compared to the East Siberian Sea, as the terrOC input of the later is dominated by deeper carbon sources via coastal erosion, whereas the main terrOC supply for the Laptev Sea transect is delivered by the Lena River (Bröder et al., 2018; Keskitalo et al., 2017; Tesi, Muschitiello, et al., 2016; Vonk et al., 2012). However, for both parts of this shelf system, regardless whether terrOC sources are governed by coastal erosion or river discharge, similarly large across-shelf gradients for OC and terrestrial biomarkers have been observed previously (Tesi, Semiletov, et al., 2016).

The other derived parameters were similar, with the initial loading $I_{\text{deg}} = 1.2 \pm 0.1 \text{ mg/m}^2$ ($1.4 \pm 0.4 \text{ mg/m}^2$ in Bröder et al., 2018) and the recalcitrant residue $R = 0.15 \pm 0.02 \text{ mg/m}^2$ ($0.21 \pm 0.02 \text{ mg/m}^2$ in Bröder et al., 2018). Some of the samples with very long transport times seem to have lower loadings than the derived recalcitrant residue R . This suggests that assuming one single degradation rate constant for a presumably complex mixture of terrOC is likely an oversimplification of the system. However, the reasonably good fit with small uncertainties for the fit parameters sustain this relatively simple method.

Dividing the part that is lost during transport (I_{deg}) by the initial loading ($I_{\text{deg}} + R$) provides an estimate of about 89% of the initial terrOC loading to be degraded. This number is in fair agreement with the degradative loss of ~85% found by Bröder et al. (2018).

Any differences may in part be due to a larger set of samples ($n = 109$ observations, distributed over 19 bins, see section 2.8, compared to $n = 10$ in the previous study), leading to slightly smaller uncertainties for these parameters. On the other hand, transport times for the East Siberian Sea are less well constrained than for

the Laptev Sea. Here it was assumed that the cross-shelf transport in the East Siberian Sea scales linearly with water depth as observed for the Laptev Sea (Bröder et al., 2018). However, sediment transport processes may differ since the freshwater input to the eastern part of the LS + ESS does not come from one overwhelming source as the Lena River in the western part. Depending on the prevailing atmospheric conditions, sediment transport may be dominated by the Siberian Coastal current and thus occur not across but rather along the shelf (Weingartner et al., 1999). The inflow of Pacific waters, east of 160°E, may further affect sediment transport processes (Semiletov et al., 2005; Steele & Ermold, 2004). The overall relatively small uncertainties for the derived parameters (root-mean-square deviation of 0.063), however, support this approach and thus the assumption of a linear relationship between water depth and transport time for the entire LS + ESS study area.

4.3. Degradable terrOC in Laptev and East Siberian Sea Surface Sediments

Next, we used the data presented in the previous sections to quantify an inventory for the terrOC pool currently available in surface sediments across the LS + ESS that is prone to degradation during cross-shelf transport, that is, the degradable terrOC fraction. First, we determined the total concentration of terrOC C_{terrOC} (in mg/gdw) in the mobile sediments (<63- μm grain size; as in section 4.1 and Figure 4b) and subtracted the part that is recalcitrant thereof. The amount of recalcitrant terrOC C_{recal} (in mg/gdw) is calculated from the asymptotic value R (in mg/m^2 , see section 4.2) and the mineral surface area (SA , in m^2/gdw) for each sample as

$$C_{\text{recal}} = R \times SA \quad (5)$$

The fraction of degradable terrOC, C_{deg} , is then calculated by difference from the total terrOC

$$C_{\text{deg}} = C_{\text{terrOC}} - C_{\text{recal}} \quad (6)$$

The concentrations of degradable terrOC span from 0 to 12 mg/gdw (Figure 4c and Table S2 in the supporting information). They are highest close to the Lena River delta and below 3 mg/gdw for most of the broader shelf.

4.4. Degradable terrOC Inventory and Carbon Flux From the Surficial Sediments

The inventory of degradable terrOC is calculated as the concentration of terrOC at each sampling station integrated over the area enclosed by the samples, see Figure 4c.

$$I_{\text{deg}} = \int_{\text{Area}} C_{\text{deg}}(\text{lon}, \text{lat}) \times \rho_{\text{sed}} \times (1 - \Phi) \times z_{\text{mix}} \, d\text{lon} \, d\text{lat} \quad (7)$$

Here $C_{\text{deg}}(\text{long}, \text{lat})$ is the concentration of degradable terrOC (i.e., recalcitrant subtracted from the total) in the mobile sediment fraction at location (lon, lat) in grams per gram dry weight as defined in the previous section 4.3 and assumed to be constant over the depth of the mixed layer, z_{mix} , ρ_{sed} is the sediment density in grams per cubic centimeters and Φ is the (dimensionless) average porosity over the depth of the mixed layer, z_{mix} , in centimeters. Concentrations of terrOC were determined for discrete surface sediment samples by $\delta^{13}\text{C}$ -based source apportionment and then interpolated over the covered area (see sections 2.6 and 2.9). For the sediment mineral density, the commonly used average of $\rho_{\text{sed}} = 2.5 \pm 0.25 \text{ g}/\text{cm}^3$ (Jönsson et al., 2003, and citations therein) was assumed here, as the exact proportions of clay ($\rho_{\text{clay}} = 2\text{--}2.6 \text{ g}/\text{cm}^3$), quartz ($\rho_{\text{quartz}} = 2.65 \text{ g}/\text{cm}^3$), and feldspar ($\rho_{\text{feldspar}} = 2.6\text{--}2.75 \text{ g}/\text{cm}^3$) are unknown for the study area. The sediment porosity Φ was analyzed for $n = 9$ sediment cores across the Laptev Sea (see Table S1 for exact locations). These measurements were averaged over the mixing depth. The mean value of all cores $\Phi = 0.7 \pm 0.09$ was used in this study. This result agrees with earlier compilations (e.g., Emerson & Hedges, 1988; Hedges & Oades, 1997). The mixed layer depth z_{mix} was determined from the lead (Pb) concentrations measured by XRF for four sediment cores (see Table S1 for exact locations). In the mixed layer, values were generally higher due to recent atmospheric input from fuel combustion (Macdonald et al., 2000) and decreased below ~4 cm (the Russian Federation banned the use of leaded gasoline nationwide in 2002). The X-ray images obtained from the same method showed an increase in the wet bulk density, that is, decrease in porosity, at ~4 cm as well (see Figure S1 for one representative station). From ^{210}Pb measurements no clear mixed layer was discernible. Taken together, we therefore take z_{mix} to be $4 \pm 1 \text{ cm}$ for this system. This value is

rather low compared to the global average of 9.8 ± 4.5 cm compiled by Boudreau (1994). For that study, previously published data of mixed layer depths (determined with several different radio-isotopic methods, see Boudreau (1994) and citations therein) were collected for >200 cores from different coastal, shelf, and deep sea environments. Their compilation, however, is lacking cores from the Arctic shelves.

With these parameters, the inventory of degradable terrOC (I_{deg}) in surface sediments of the LS + ESS was estimated to 0.64 ± 0.28 Tg using equation (7). Since the area covered here only accounts for 55% of the total LS + ESS, the best estimate (without any additional information) was to assume a similar average concentration of degradable terrOC for the entire Laptev and East Siberian shelves. The inventory for the whole area was then calculated as (0.64 ± 0.28) Tg/ $0.55 \approx 1.2 \pm 0.53$ Tg.

The carbon flux F_{deg} (in g/year) emerging from degradation of terrOC in surface sediments across the LS + ESS is quantified by multiplying the inventory of degradable terrOC I_{deg} with the first-order terrOC degradation rate constant k of 0.0015 ± 0.0002 per year (see Figure 5):

$$F_{deg} = I_{deg} \times k \quad (8)$$

This calculation yielded a flux of degraded terrOC at about 1.7 ± 0.97 Gg (=1,700 ± 970 t) carbon per year for the surficial sediments of the LS + ESS.

4.5. Comparison of terrOC Degradation in Surficial Sediments to Other Carbon Fluxes on the Laptev and East Siberian Sea Shelves

The carbon flux from terrOC degradation in the surficial sediments was compared with other major flux vectors for terrOC in this extensive shelf-sea system. These include carbon fluxes from degradation of DOC and POC, the total outgassing caused by terrOC degradation (measured as net CO₂ released to the atmosphere), and land-ocean input and burial fluxes in the sediments.

The size of the total inventory for DOC was estimated to be 94 Tg, with a large portion of this pool being of riverine origin, based on correlations with salinity (Alling et al., 2010). However, we note that this DOC inventory estimate is at odds with the yearly DOC delivery by Lena and Kolyma Rivers combined (~ 6.5 Tg C year⁻¹; Holmes et al., 2012) and the estimated shelf water residence time of ~ 3.5 years (Alling et al., 2010, and citations therein). Since the DOC release by coastal erosion is comparably small (e.g., Sánchez-García et al., 2011), the contribution from marine primary production might be rather substantial. For DOC in the western East Siberian Sea (west of 160°E), a first-order removal rate was found to be ~ 0.3 year⁻¹ (Alling et al., 2010). A similar rate may hold for the entire LS + ESS, but for the Laptev Sea, freshwater residence times were too short and for the eastern East Siberian Sea, they were too poorly constrained to obtain a removal rate. The net DOC removal flux for the western East Siberian Sea was quantified to ~ 5.1 Tg C year⁻¹ (Alling et al., 2010).

The POC inventory for the entire LS + ESS added up to 4.2 ± 0.3 Tg, with ~ 1.8 Tg for the Laptev and ~ 2.4 Tg for the East Siberian Sea (Sánchez-García et al., 2011). From the depleted $\delta^{13}C$ signal for POC from the Laptev and western East Siberian Sea it was assumed that this was mainly terrigenous, while for the ~ 2.4 Tg from the eastern East Siberian Sea, a contribution of about 50% terrOC was estimated (Sánchez-García et al., 2011). Thus, an inventory of ~ 3 Tg terrigenous POC results for the entire LS + ESS.

For POC a first-order degradation rate was constrained to be 1.4 ± 0.9 year⁻¹ for the Laptev Sea and the western East Siberian Sea (west of 160°E; Sánchez-García et al., 2011). As these areas of the LS + ESS were dominated by terrigenous POC, the rate is assumed to apply to particulate terrOC (if the inventory included marine POC, the degradation rate constant would be underestimated). No degradation rate constant was derived for the eastern part of the East Siberian Sea (east of 160°E) due to uncertainties regarding the likely much larger marine contribution to the POC inventory in this area. The removal flux for terrigenous POC degradation in the Laptev and western East Siberian Sea was thus assessed by a steady state mass balance to be ~ 2.5 Tg C year⁻¹, accounting for sediment burial and net hydraulic exchange (Sánchez-García et al., 2011).

For inventory comparisons the total amount of terrOC in surface sediments should be taken into account (instead of only the degradable fraction). The size of the terrOC inventory I_{terrOC} (calculated in analogy to I_{deg} , but using $C_{terrOC}(\text{lon}, \text{lat})$ instead of $C_{deg}(\text{lon}, \text{lat})$ in equation (7)) is with $\sim 2.7 \pm 0.84$ Tg about double

the size of I_{deg} and similar to the size of the POC inventory (Sánchez-García et al., 2011). The inventory for total sedimentary OC I_{OC} (calculated accordingly, exchanging $C_{\text{deg}}(\text{lon, lat})$ with $C_{\text{OC}}(\text{lon, lat})$ in equation (7)) sums up to $\sim 3.8 \pm 1.1$ Tg, approximately three times the size of I_{deg} , but still about a factor of 25 smaller than the total amount of DOC suggested for the LS + ESS (Alling et al., 2010).

The degradation rate constant for sedimentary terrOC is with 0.0015 year^{-1} 2–3 orders of magnitude smaller than the ones for water column POC and DOC on the LS + ESS. This difference may in part be due to less oxygen availability in the sediments. Since the oxygen penetration depths for LS + ESS sediments is on the order of a few millimeters (Boetius & Damm, 1998; Brüchert et al., 2018), the average oxygen exposure time for the mixed layer (~ 4 cm) is much lower than the sedimentary cross-shelf transport time. POC and DOC in oxygenated waters, in contrast, are exposed to oxygen at all times. Another protective mechanism against degradation for sedimentary terrOC may be the close interaction with the mineral surfaces of the sediments through sorption (Hedges & Keil, 1995; Keil et al., 1994; Mayer, 1994b). Also, sediments may contain a higher proportion of intrinsically refractory organic matter (kerogen), which is not soluble in water (Zonneveld et al., 2010).

The current study provides constraints to quantitatively demonstrate that the carbon released from terrOC degradation in LS + ESS surface sediments ($1.7 \pm 0.97 \text{ Gg C year}^{-1}$) is 3–4 orders of magnitude smaller than the estimates for terrigenous DOC and POC degradation in the LS + ESS water column. The major fraction of the $15\text{--}30 \text{ Tg C year}^{-1}$ terrOC that is delivered to LS + ESS as POC through coastal erosion and river discharge (combined estimates from Vonk et al., 2012; McClelland et al., 2016) appears to get buried in the sediments ($20\text{--}30 \text{ Tg C year}^{-1}$, Vonk et al., 2012).

According to our findings, degradation in the top few cm of the sediment thus appears to contribute only a minor fraction to the total $\sim 10 \text{ Tg C year}^{-1}$ of carbon that is released as CO_2 to the atmosphere from terrOC degradation on the Siberian shelves (Anderson et al., 2009). The anticipated total carbon flux released from thawing permafrost soils of the whole circumpolar Arctic landscape is yet several orders of magnitude larger, though conflicted with a high degree of uncertainty. One reason why these emissions are so poorly constrained is the fact that lateral carbon fluxes and the role of spatially and temporally displaced feedbacks are currently not properly represented in most estimates (Schoor et al., 2015; Vonk & Gustafsson, 2013), an aspect we are trying to partially alleviate with the current study. Admittedly, our approach is not accounting for the degradation of terrOC in resuspended sediment/bottom floc occurring at the water-sediment interface, which have been observed indirectly by, for example, Semiletov et al. (2016). Sedimentary terrOC degradation below the mixing layer by anaerobic degradation is low ($<20\%$ of the depth-integrated bulk carbon mineralization according to Brüchert et al., 2018, which is consistent with downcore profiles of terrOC and biomarker concentrations in Bröder, Tesi, Salvadó, et al., 2016). Therefore, deposition of terrOC in the sediments may function as a removal mechanism for permafrost-released OC from the contemporary carbon cycle. With ongoing climate change leading to, for example, shrinking sea ice cover, increasing terrOC delivery, and potentially enhanced primary production, these numbers are also likely subject to change over the coming decades to century.

5. Summary and Conclusions

This study comprises the first inventory of terrOC for surface sediments covering the LS + ESS, the World's largest shelf sea system. The size of the terrOC reservoir in the mixed surface sediment layer (top 4 cm) was estimated to be $\sim 2.7 \pm 0.84$ Tg, which makes up about 70% of the total OC present in LS + ESS surface sediments. Approximately 55% of the terrOC pool currently present in the surface sediments was found to be recalcitrant on the order of several millennia; on the outer shelf almost all terrOC was made up of recalcitrant residue. The degradable fraction ($\sim 1.2 \pm 0.53$ Tg) decayed following a first-order degradation rate constant of $1.5 \pm 0.2 \text{ kyr}^{-1}$. This approximation is the average for the whole terrOC pool in the surficial sediments; different carbon subpools likely have different degradation rates. It has also been demonstrated that there is more degradation taking place in the nearshore zone, decreasing with distance from the coast. However, this study provides a first estimate for the full compartment of this shelf sea system. From these results, the flux originating from terrOC degradation in the LS + ESS surface sediments was quantitatively constrained to be around $1.7 \pm 0.97 \text{ Gg/year}$. A comparison with terrOC degradation in water column DOC and POC phases showed that the contribution from the surface sediments to the total terrOC degradation is

several orders of magnitude smaller than from the other compartments. This is largely due to the substantially lower degradation rate constant (a factor 200–930 smaller than for DOC and POC). Still, a number of uncertainties prevail: the sediment sample coverage on the midshelf for the East Siberian Sea is sparse and data are lacking entirely for the western Laptev Sea and the eastern East Siberian Sea. Better assessments of sediment transport times for the East Siberian Sea could potentially change the degradation rate constant and the estimate for the recalcitrant residue; the first would influence the flux calculation, while the latter would modify the size of the inventory of degradable terrOC. Nevertheless, all these values are unlikely to be off by more than a factor of 2; therefore, even when taking all uncertainties into account, the carbon flux from terrOC degradation in the surface sediments would still only be a minor contribution to the total carbon released from terrOC degradation on the Laptev and East Siberian Sea shelves. Taken that anaerobic degradation in deeper compartments of the sediment is low, these results imply that the burial of permafrost-released terrOC in marine sediments may serve as an important mechanism to attenuate potential permafrost carbon-climate feedbacks.

Acknowledgments

We thank crew and personnel of the RV Yakob Smirnitskiy, the TB0012, and the IB ODEN. The International Siberian Shelf Study 2008 (ISSS-08) and the SWERUS-C3 2014 expeditions were supported by the Knut and Alice Wallenberg Foundation, Headquarters of the Far Eastern Branch of the Russian Academy of Sciences, the Swedish Research Council (VR contract 621-2007-4631, 621-2013-5297, and 2017-05687), the European Research Council (ERC-AdG CC-TOP project 695331 to Ö. G.), the US National Oceanic and Atmospheric Administration (OAR Climate Program Office, NA08OAR4600758/Siberian Shelf Study), the Swedish Polar Research Secretariat, the Nordic Council of Ministers, and the U.S. National Science Foundation (OPP ARC-0909546 and 1023281). L. B. and Ö. G. also acknowledge financial support from the Climate Research School of the Bolin Centre for Climate Research. T. T. also acknowledges EU financial support as a Marie Curie fellow (contract PIEF-GA-2011-300259), contribution number 1988 of ISMAR-CNR Sede di Bologna. I. S. further thanks the Russian Government for financial support (megagrant 14.Z50.31.0012). Aron Varhelyi contributed valuable support with laboratory work. All data used in this study are provided in the supporting information as Tables S1–S3. They can also be found as Excel files at the Bolin Centre Database (<https://bolin.su.se/data/Broder-2019>).

References

- Alling, V., Sanchez-Garcia, L., Porcelli, D., Pugach, S., Vonk, J. E., Van Dongen, B., et al. (2010). Nonconservative behavior of dissolved organic carbon across the Laptev and East Siberian seas. *Global Biogeochemical Cycles*, *24*, GB4033. <https://doi.org/10.1029/2010GB003834>
- Amon, R. M. W., Rinehart, A. J., Duan, S., Louchouart, P., Prokushkin, A., Guggenberger, G., et al. (2012). Dissolved organic matter sources in large Arctic rivers. *Geochimica et Cosmochimica Acta*, *94*, 217–237. <https://doi.org/10.1016/j.gca.2012.07.015>
- Anderson, L. G., Björk, G., Jutterström, S., Pipko, I., Shakhova, N., Semiletov, I., & Wahlström, I. (2011). East Siberian Sea, an Arctic region of very high biogeochemical activity. *Biogeosciences*, *8*(6), 1745–1754. <https://doi.org/10.5194/bg-8-1745-2011>
- Anderson, L. G., Jutterström, S., Hjalmarsson, S., Wahlström, I., & Semiletov, I. P. (2009). Out-gassing of CO₂ from Siberian Shelf seas by terrestrial organic matter decomposition. *Geophysical Research Letters*, *36*, L20601. <https://doi.org/10.1029/2009GL040046>
- Belicka, L. L., & Harvey, H. R. (2009). The sequestration of terrestrial organic carbon in Arctic Ocean sediments: A comparison of methods and implications for regional carbon budgets. *Geochimica et Cosmochimica Acta*, *73*(20), 6231–6248. <https://doi.org/10.1016/j.gca.2009.07.020>
- Bischoff, J., Sparkes, R. B., Doğrul Selver, A., Spencer, R. G. M., Gustafsson, Ö., Semiletov, I. P., et al. (2016). Source, transport and fate of soil organic matter inferred from microbial biomarker lipids on the East Siberian Arctic Shelf. *Biogeosciences*, *13*(17), 4899–4914. <https://doi.org/10.5194/bg-13-4899-2016>
- Blair, N. E., & Aller, R. C. (2012). The fate of terrestrial organic carbon in the marine environment. *Annual Review of Marine Science*, *4*(1), 401–423. <https://doi.org/10.1146/annurev-marine-120709-142717>
- Boetius, A., & Damm, E. (1998). Benthic oxygen uptake, hydrolytic potentials and microbial biomass at the Arctic continental slope. *Deep-Sea Research Part I: Oceanographic Research Papers*, *45*(2–3), 239–275. [https://doi.org/10.1016/S0967-0637\(97\)00052-6](https://doi.org/10.1016/S0967-0637(97)00052-6)
- Boudreau, B. P. (1994). Is burial velocity a master parameter for bioturbation? *Geochimica et Cosmochimica Acta*, *58*(4), 1243–1249. [https://doi.org/10.1016/0016-7037\(94\)90378-6](https://doi.org/10.1016/0016-7037(94)90378-6)
- Bröder, L., Tesi, T., Andersson, A., Eglinton, T. I., Semiletov, I. P., Dudarev, O. V., et al. (2016). Historical records of organic matter supply and degradation status in the east Siberian Sea. *Organic Geochemistry*, *91*, 16–30. <https://doi.org/10.1016/j.orggeochem.2015.10.008>
- Bröder, L., Tesi, T., Andersson, A., Semiletov, I., & Gustafsson, Ö. (2018). Bounding the role of cross-shelf transport and degradation in land-ocean carbon transfer. *Nature Communications*, *9*(1), 806. <https://doi.org/10.1038/s41467-018-03192-1>
- Bröder, L., Tesi, T., Salvadó, J. A., Semiletov, I. P., Dudarev, O. V., & Gustafsson, Ö. (2016). Fate of terrigenous organic matter across the Laptev Sea from the mouth of the Lena River to the deep sea of the Arctic interior. *Biogeosciences*, *13*(17), 5003–5019. <https://doi.org/10.5194/bg-13-5003-2016>
- Brüchert, V., Bröder, L., Sawicka, J. E., Tesi, T., Joye, S. P., Sun, X., et al. (2018). Carbon mineralization in Laptev and East Siberian sea shelf and slope sediment. *Biogeosciences*, *15*(2), 471–490. <https://doi.org/10.5194/bg-15-471-2018>
- Brunauer, S., Emmett, P. H., & Teller, E. (1938). Adsorption of gases in multimolecular layers. *Journal of the American Chemical Society*, *60*(2), 309–319. <https://doi.org/citeulike-article-id:4074706> <https://doi.org/10.1021/ja01269a023>
- Charkin, A. N., Dudarev, O. V., Semiletov, I. P., Kruhmaliev, A. V., Vonk, J. E., Sánchez-García, L., et al. (2011). Seasonal and interannual variability of sedimentation and organic matter distribution in the Buor-Khaya Gulf: The primary recipient of input from Lena River and coastal erosion in the southeast Laptev Sea. *Biogeosciences*, *8*(9), 2581–2594. <https://doi.org/10.5194/bg-8-2581-2011>
- Dethleff, D. (2005). Entrainment and export of Laptev Sea ice sediments, Siberian Arctic. *Journal of Geophysical Research*, *110*, C07009. <https://doi.org/10.1029/2004JC002740>
- Dethleff, D. (2010). Dense water formation in the Laptev Sea flaw lead. *Journal of Geophysical Research*, *115*, C12022. <https://doi.org/10.1029/2009JC006080>
- Dmitrenko, I. A., Kirillov, S. A., & Bruno Tremblay, L. (2008). The long-term and interannual variability of summer fresh water storage over the eastern Siberian shelf: Implication for climatic change. *Journal of Geophysical Research*, *113*, C03007. <https://doi.org/10.1029/2007JC004304>
- Doğrul Selver, A., Sparkes, R. B., Bischoff, J., Talbot, H. M., Gustafsson, Ö., Semiletov, I. P., et al. (2015). Distributions of bacterial and archaeal membrane lipids in surface sediments reflect differences in input and loss of terrestrial organic carbon along a cross-shelf Arctic transect. *Organic Geochemistry*, *83–84*, 16–26. <https://doi.org/10.1016/j.orggeochem.2015.01.005>
- Eicken, H., Reimnitz, E., Alexandrov, V., Martin, T., Kassens, H., & Viehoff, T. (1997). Sea-ice processes in the Laptev Sea and their importance for sediment export. *Continental Shelf Research*, *17*(2), 205–233. [https://doi.org/10.1016/S0278-4343\(96\)00024-6](https://doi.org/10.1016/S0278-4343(96)00024-6)
- Emerson, S., & Hedges, J. I. (1988). Processes controlling the organic carbon content of open ocean sediments. *Paleoceanography*, *3*(5), 621–634. <https://doi.org/10.1029/PA003i005p00621>
- Fahl, K., & Stein, R. (1997). Modern organic carbon deposition in the Laptev Sea and the adjacent continental slope: Surface water productivity vs. terrigenous input. *Organic Geochemistry*, *26*(5–6), 379–390. [https://doi.org/10.1016/S0146-6380\(97\)00007-7](https://doi.org/10.1016/S0146-6380(97)00007-7)

- Fry, B., & Sherr, E. B. (1984). $\delta^{13}\text{C}$ measurements as indicators of carbon flow in marine and freshwater ecosystems. *Contributions in Marine Science*, 27, 13–49.
- Goni, M. A., O'Connor, A. E., Kuzyk, Z. Z., Yunker, M. B., Gobeil, C., & Macdonald, R. W. (2013). Distribution and sources of organic matter in surface marine sediments across the North American Arctic margin. *Journal of Geophysical Research: Oceans*, 118, 4017–4035. <https://doi.org/10.1002/jgrc.20286>
- Gordeev, V. V. (2006). Fluvial sediment flux to the Arctic Ocean. *Geomorphology*, 80(1–2), 94–104. <https://doi.org/10.1016/j.geomorph.2005.09.008>
- Guay, C. K. H., Falkner, K. K., Muench, R. D., Mensch, M., Frank, M., & Bayer, R. (2001). Wind-driven transport for Eurasian Arctic river discharge. *Journal of Geophysical Research*, 106(C6), 11,469–11,480. <https://doi.org/10.1029/2000JC000261>
- Günther, F., Overduin, P. P., Sandakov, A. V., Grosse, G., & Grigoriev, M. N. (2013). Short- and long-term thermo-erosion of ice-rich permafrost coasts in the Laptev Sea region. *Biogeosciences*, 10(6), 4297–4318. <https://doi.org/10.5194/bg-10-4297-2013>
- Hedges, J. I., & Keil, R. G. (1995). Sedimentary organic matter preservation: An assessment and speculative synthesis. *Marine Chemistry*, 49(2–3), 81–115. [https://doi.org/10.1016/0304-4203\(95\)00008-F](https://doi.org/10.1016/0304-4203(95)00008-F)
- Hedges, J. I., & Oades, J. M. (1997). Comparative organic geochemistries of soils and marine sediments. *Organic Geochemistry*, 27(7–8), 319–361. [https://doi.org/10.1016/S0146-6380\(97\)00056-9](https://doi.org/10.1016/S0146-6380(97)00056-9)
- Hilton, R. G., Galy, V., Gaillardet, J., Dellinger, M., Bryant, C., O'Regan, M., et al. (2015). Erosion of organic carbon in the Arctic as a geological carbon dioxide sink. *Nature*, 524(7563), 84–87. <https://doi.org/10.1038/nature14653>
- Holmes, R. M., McClelland, J. W., Peterson, B. J., Tank, S. E., Buluygina, E., Eglinton, T. I., et al. (2012). Seasonal and annual fluxes of nutrients and organic matter from large rivers to the Arctic Ocean and surrounding seas. *Estuaries and Coasts*, 35(2), 369–382. <https://doi.org/10.1007/s12237-011-9386-6>
- Hugelius, G., Strauss, J., Zubrzycki, S., Harden, J. W., Schuur, E. A. G., Ping, C.-L., et al. (2014). Estimated stocks of circumpolar permafrost carbon with quantified uncertainty ranges and identified data gaps. *Biogeosciences*, 11(23), 6573–6593. <https://doi.org/10.5194/bg-11-6573-2014>
- Intergovernmental Panel on Climate Change (2013). In T. F. Stocker et al. (Eds.), *Climate Change 2013: The Physical Science Basis. Contribution of Working Group I to the Fifth Assessment Report of the Intergovernmental Panel on Climate Change*. Cambridge, UK and New York: Cambridge University Press.
- Ivanov, V. V., & Golovin, P. N. (2007). Observations and modeling of dense water cascading from the northwestern Laptev Sea shelf. *Journal of Geophysical Research*, 112, C09003. <https://doi.org/10.1029/2006JC003882>
- Jakobsson, M., Grantz, A., Kristoffersen, Y., & Macnab, R. (2004). Physiography and bathymetry of the Arctic Ocean. In R. Stein & R. W. Macdonald (Eds.), *The organic carbon cycle in the Arctic Ocean* (pp. 1–5). Berlin Heidelberg: Springer-Verlag.
- Jönsson, A., Gustafsson, Ö., Axelman, J., & Sundberg, H. (2003). Global accounting of PCBs in the continental shelf sediments. *Environmental Science & Technology*, 37(2), 245–255. <https://doi.org/10.1021/es0201404>
- Karlsson, E. S., Brüchert, V., Tesi, T., Charkin, A., Dudarev, O., Semiletov, I., & Gustafsson, Ö. (2014). Contrasting regimes for organic matter degradation in the East Siberian Sea and the Laptev Sea assessed through microbial incubations and molecular markers. *Marine Chemistry*, 170, 11–22. <https://doi.org/10.1016/j.marchem.2014.12.005>
- Karlsson, E. S., Charkin, A., Dudarev, O., Semiletov, I., Vonk, J. E., Sánchez-García, L., & Andersson, A. (2011). Carbon isotopes and lipid biomarker investigation of sources, transport and degradation of terrestrial organic matter in the Buor-Khaya Bay, SE Laptev Sea. *Biogeosciences*, 8(7), 1865–1879. <https://doi.org/10.5194/bg-8-1865-2011>
- Keil, R. G., Dickens, A. F., Arnarson, T., Nunn, B. L., & Devol, A. H. (2004). What is the oxygen exposure time of laterally transported organic matter along the Washington margin? *Marine Chemistry*, 92(1–4), 157–165. <https://doi.org/10.1016/j.marchem.2004.06.024>
- Keil, R. G., Tsamakis, E., Fuh, C. B., Giddings, J. C., & Hedges, J. I. (1994). Mineralogical and textural controls on the organic composition of coastal marine sediments: Hydrodynamic separation using SPLITT-fractionation. *Geochimica et Cosmochimica Acta*, 58(2), 879–893. [https://doi.org/10.1016/0016-7037\(94\)90512-6](https://doi.org/10.1016/0016-7037(94)90512-6)
- Keskitalo, K., Tesi, T., Bröder, L., Andersson, A., Pearce, C., Sköld, M., et al. (2017). Sources and characteristics of terrestrial carbon in Holocene-scale sediments of the East Siberian Sea. *Climate of the Past*, 13(9), 1213–1226. <https://doi.org/10.5194/cp-13-1213-2017>
- Macdonald, R. W., Barrie, L. A., Bidleman, T. F., Diamond, M. L., Gregor, D. J., Semkin, R. G., et al. (2000). Contaminants in the Canadian Arctic: 5 years of progress in understanding sources, occurrence and pathways. *Science of the Total Environment*, 254(2–3), 93–234. [https://doi.org/10.1016/S0048-9697\(00\)00434-4](https://doi.org/10.1016/S0048-9697(00)00434-4)
- Mayer, L. M. (1994a). Relationships between mineral surfaces and organic carbon concentrations in soils and sediments. *Chemical Geology*, 114(3–4), 347–363. [https://doi.org/10.1016/0009-2541\(94\)90063-9](https://doi.org/10.1016/0009-2541(94)90063-9)
- Mayer, L. M. (1994b). Surface area control of organic carbon accumulation in continental shelf sediments. *Geochimica et Cosmochimica Acta*, 58(4), 1271–1284. [https://doi.org/10.1016/0016-7037\(94\)90381-6](https://doi.org/10.1016/0016-7037(94)90381-6)
- McClelland, J. W., Déry, S. J., Peterson, B. J., Holmes, R. M., & Wood, E. F. (2006). A pan-arctic evaluation of changes in river discharge during the latter half of the 20th century. *Geophysical Research Letters*, 33, L06715. <https://doi.org/10.1029/2006GL025753>
- McClelland, J. W., Holmes, R. M., Peterson, B. J., Raymond, P. A., Striegl, R. G., Zhulidov, A. V., et al. (2016). Particulate organic carbon and nitrogen export from major Arctic rivers. *Global Biogeochemical Cycles*, 30, 629–643. <https://doi.org/10.1002/2015GB005351>
- Mollenhauer, G., Inthorn, M., Vogt, T., Zabel, M., Sinninghe Damsté, J. S., & Eglinton, T. I. (2007). Aging of marine organic matter during cross-shelf lateral transport in the Benguela upwelling system revealed by compound-specific radiocarbon dating. *Geochemistry, Geophysics, Geosystems*, 8, Q09004. <https://doi.org/10.1029/2007GC001603>
- Naidu, A. S., Cooper, L. W., Finney, B. P., Macdonald, R. W., Alexander, C., & Semiletov, I. P. (2000). Organic carbon isotope ratio ($\delta^{13}\text{C}$) of Arctic Amerasian Continental shelf sediments. *International Journal of Earth Sciences*, 89(3), 522–532. <https://doi.org/10.1007/s005310000121>
- Nieuwenhuize, J., Maas, Y. E., & Middelburg, J. J. (1994). Rapid analysis of organic carbon and nitrogen in particulate materials. *Marine Chemistry*, 45(3), 217–224. [https://doi.org/10.1016/0304-4203\(94\)90005-1](https://doi.org/10.1016/0304-4203(94)90005-1)
- Rachold, V., Eicken, H., Gordeev, V. V., Grigoriev, M. N., Hubberten, H.-W., Lisitzin, A. P., et al. (2004). Modern terrigenous organic carbon input to the Arctic Ocean. In R. Stein & R. W. Macdonald (Eds.), *The Organic Carbon Cycle in the Arctic Ocean* (pp. 33–55). Berlin, Heidelberg: Springer. https://doi.org/10.1007/978-3-642-18912-8_2
- Sakshaug, E. (2004). Primary and secondary production in the Arctic Seas. In R. Stein & R. W. Macdonald (Eds.), *The organic carbon cycle in the Arctic Ocean* (pp. 57–81). Berlin, Heidelberg: Springer. <https://doi.org/10.1007/978-3-642-18912-8>
- Salvadó, J. A., Tesi, T., Sundbom, M., Karlsson, E., Kruså, M., Semiletov, I. P., et al. (2016). Contrasting composition of terrigenous organic matter in the dissolved, particulate and sedimentary organic carbon pools on the outer East Siberian Arctic Shelf. *Biogeosciences*, 13(22), 6121–6138. <https://doi.org/10.5194/bg-13-6121-2016>

- Sánchez-García, L., Alling, V., Pugach, S., Vonk, J., Van Dongen, B., Humborg, C., et al. (2011). Inventories and behavior of particulate organic carbon in the Laptev and East Siberian seas. *Global Biogeochemical Cycles*, 25, GB2007. <https://doi.org/10.1029/2010GB003862>
- Savelieva, N. I., Semiletov, I. P., Vasilevskaya, L. N., & Pugach, S. P. (2000). A climate shift in seasonal values of meteorological and hydrological parameters for northeastern Asia. *Progress in Oceanography*, 47(2–4), 279–297. [https://doi.org/10.1016/S0079-6611\(00\)00039-2](https://doi.org/10.1016/S0079-6611(00)00039-2)
- Schuur, E. A. G., McGuire, A. D., Grosse, G., Harden, J. W., Hayes, D. J., Hugelius, G., et al. (2015). Climate change and the permafrost carbon feedback. *Nature*, 520(7546), 171–179. <https://doi.org/10.1038/nature14338>
- Semiletov, I., Dudarev, O., Luchin, V., Charkin, A., Shin, K. H., & Tanaka, N. (2005). The East Siberian Sea as a transition zone between Pacific-derived waters and Arctic shelf waters. *Geophysical Research Letters*, 32, L10614. <https://doi.org/10.1029/2005GL022490>
- Semiletov, I., Makshtas, A., Akasofu, S. I., & Andreas, E. L. (2004). Atmospheric CO₂ balance: The role of Arctic sea ice. *Geophysical Research Letters*, 31, L05121. <https://doi.org/10.1029/2003GL017996>
- Semiletov, I., Pipko, I., Gustafsson, Ö., Anderson, L. G., Sergienko, V., Pugach, S., et al. (2016). Acidification of East Siberian Arctic Shelf waters through addition of freshwater and terrestrial carbon. *Nature Geoscience*, 9(5), 361–365. <https://doi.org/10.1038/ngeo2695>
- Semiletov, I. P. (1999). Destruction of the coastal permafrost ground as an important factor in biogeochemistry of the Arctic Shelf waters. *Transactions [Doklady] of Russian Academy of Sciences*, 368(6), 679–682.
- Semiletov, I. P., Pipko, I. I., Repina, I., & Shakhova, N. E. (2007). Carbonate chemistry dynamics and carbon dioxide fluxes across the atmosphere–ice–water interfaces in the Arctic Ocean: Pacific sector of the Arctic. *Journal of Marine Systems*, 66(1–4), 204–226. <https://doi.org/10.1016/j.jmarsys.2006.05.012>
- Semiletov, I. P., Pipko, I. I., Shakhova, N. E., Dudarev, O. V., Pugach, S. P., Charkin, a. N., et al. (2011). Carbon transport by the Lena River from its headwaters to the Arctic Ocean, with emphasis on fluvial input of terrestrial particulate organic carbon vs. carbon transport by coastal erosion. *Biogeosciences*, 8(9), 2407–2426. <https://doi.org/10.5194/bg-8-2407-2011>
- Semiletov, I. P., Shakhova, N. E., Sergienko, V. I., Pipko, I. I., & Dudarev, O. V. (2012). On carbon transport and fate in the East Siberian Arctic land–shelf–atmosphere system. *Environmental Research Letters*, 7(1), 015201. <https://doi.org/10.1088/1748-9326/7/1/015201>
- Shakhova, N., Semiletov, I., Sergienko, V., Lobkovsky, L., Yusupov, V., Salyuk, A., et al. (2015). The East Siberian Arctic Shelf: Towards further assessment of permafrost-related methane fluxes and role of sea ice. *Philosophical Transactions. Series A, Mathematical, Physical, and Engineering Sciences*, 373(2052), 20140451. <https://doi.org/10.1098/rsta.2014.0451>
- Sparkes, R. B., Doğrul Selver, A., Bischoff, J., Talbot, H. M., Gustafsson, Ö., Semiletov, I. P., et al. (2015). GDGT distributions on the East Siberian Arctic Shelf: Implications for organic carbon export, burial and degradation. *Biogeosciences*, 12(12), 3753–3768. <https://doi.org/10.5194/bg-12-3753-2015>
- Sparkes, R. B., Doğrul Selver, A., Gustafsson, Ö., Semiletov, I. P., Haghypour, N., Wacker, L., et al. (2016). Macromolecular composition of terrestrial and marine organic matter in sediments across the East Siberian Arctic Shelf. *The Cryosphere*, 10(5), 2485–2500. <https://doi.org/10.5194/tc-10-2485-2016>
- Steele, M., & Ermold, W. (2004). Salinity trends on the Siberian shelves. *Geophysical Research Letters*, 31, L24308. <https://doi.org/10.1029/2004GL021302>
- Stein, R., & Fahl, K. (2004). The Laptev Sea: Distribution, sources, variability and burial of organic carbon. In R. Stein & R. W. Macdonald (Eds.), *The organic carbon cycle in the Arctic Ocean* (pp. 213–236). Berlin Heidelberg: Springer-Verlag.
- Syvitski, J. P. M. (2002). Sediment discharge variability in Arctic rivers: Implications for a warmer future. *Polar Research*, 21(2), 323–330. <https://doi.org/10.1111/j.1751-8369.2002.tb00087.x>
- Tesi, T., Geibel, M. C., Pearce, C., Panova, E., Vonk, J. E., Karlsson, E., et al. (2017). Carbon geochemistry of plankton-dominated samples in the Laptev and East Siberian shelves: Contrasts in suspended particle composition. *Ocean Science*, 13(5), 735–748. <https://doi.org/10.5194/os-13-735-2017>
- Tesi, T., Muschitiello, F., Smittenberg, R. H., Jakobsson, M., Vonk, J. E., Hill, P., et al. (2016). Massive remobilization of permafrost carbon during post-glacial warming. *Nature Communications*, 7(1), 13653. <https://doi.org/10.1038/ncomms13653>
- Tesi, T., Semiletov, I., Dudarev, O., Andersson, A., & Gustafsson, Ö. (2016). Matrix association effects on hydrodynamic sorting and degradation of terrestrial organic matter during cross-shelf transport in the Laptev and East Siberian shelf seas. *Journal of Geophysical Research: Biogeosciences*, 121, 731–752. <https://doi.org/10.1002/2015JG003067>
- Tesi, T., Semiletov, I., Hugelius, G., Dudarev, O., Kuhry, P., & Gustafsson, Ö. (2014). Composition and fate of terrigenous organic matter along the Arctic land-ocean continuum in East Siberia: Insights from biomarkers and carbon isotopes. *Geochimica et Cosmochimica Acta*, 133, 235–256. <https://doi.org/10.1016/j.gca.2014.02.045>
- Vonk, J. E., & Gustafsson, Ö. (2013). Permafrost-carbon complexities. *Nature Geoscience*, 6(9), 675–676. <https://doi.org/10.1038/ngeo1937>
- Vonk, J. E., Sánchez-García, L., Semiletov, I., Dudarev, O., Eglinton, T., Andersson, A., & Gustafsson, O. (2010). Molecular and radiocarbon constraints on sources and degradation of terrestrial organic carbon along the Kolyma paleoriver transect, East Siberian Sea. *Biogeosciences*, 7(10), 3153–3166. <https://doi.org/10.5194/bg-7-3153-2010>
- Vonk, J. E., Sánchez-García, L., van Dongen, B. E., Alling, V., Kosmach, D., Charkin, A., et al. (2012). Activation of old carbon by erosion of coastal and subsea permafrost in Arctic Siberia. *Nature*, 489(7414), 137–140. <https://doi.org/10.1038/nature11392>
- Wegner, C., Bauch, D., Hölemann, J. A., Janout, M. A., Heim, B., Novikhin, A., et al. (2013). Interannual variability of surface and bottom sediment transport on the Laptev Sea shelf during summer. *Biogeosciences*, 10(2), 1117–1129. <https://doi.org/10.5194/bg-10-1117-2013>
- Wegner, C., Hölemann, J. A., Dmitrenko, I., Kirillov, S., & Kassens, H. (2005). Seasonal variations in Arctic sediment dynamics—Evidence from 1-year records in the Laptev Sea (Siberian Arctic). *Global and Planetary Change*, 48(1–3), 126–140. <https://doi.org/10.1016/j.gloplacha.2004.12.009>
- Weingartner, T. J., Danielson, S., Sasaki, Y., Pavlov, V., & Kulakov, M. (1999). The Siberian Coastal Current: A wind- and buoyancy-forced Arctic coastal current. *Journal of Geophysical Research*, 104(C12), 29,697–29,713. <https://doi.org/10.1029/1999JC900161>
- Zonneveld, K. A. F., Versteegh, G. J. M., Kasten, S., Eglinton, T. I., Emeis, K.-C., Hugué, C., et al. (2010). Selective preservation of organic matter in marine environments; processes and impact on the sedimentary record. *Biogeosciences*, 7(2), 483–511. <https://doi.org/10.5194/bg-7-483-2010>